Pergamon

Int. J. Heat Mass Transfer. Vol. 38, No. 11, pp. 2047–2055, 1995

0017-9310/95 $9.50+0.00

0017-9310(94)00312-2

The optimal spacing between horizontal cylinders in a fixed volume cooled by natural convection

ADRIAN BEJAN

Department of Mechanical Engineering, and Materials Science, Duke University, Durham, NC 27708-0300, U.S.A.

ALEX J. FOWLER

Mechanical Engineering Department, University of Massachusetts Dartmouth, North Dartmouth, MA 02747-2300, U.S.A.

and

GEORGE STANESCU

Faculty of Mechanical Engineering, Polytechnic University of Bucharest, Bucharest 77206, Romania

(*Received* 20 *April* 1994 *and in final form* 16 *September* 1994)

Abstract—This is a theoretical, numerical and experimental study of how to select the spacing (S) between horizontal cylinders in an array with laminar natural convection, such that the total heat transfer (q) between the array and the ambient is maximized. The volume occupied by the array (height H, width W, cylinder length L) and the cylinder diameter (D) are arbitrary but fixed, while the spacing (or number of cylinders in the array) varies. The optimal spacing and maximum heat transfer results predicted theoretically are developed into accurate and well tested correlations by means of numerical simulations and experimental measurements. The recommended correlations are $S_{opt}/D = 2.72(H/D)^{1/3}Ra_D^{-1/4} + 0.263$ and $\tilde{q}_{max} = 0.448[(H/D)^{1/3}Ra_D^{-1/4}]^{-1/6}$ where $\tilde{q}_{max}$ is the dimensionless maximum overall thermal conductance, $\tilde{q}_{max} = q_{max}D^2/[HLWk(T_w - T_\infty)]$. The optimal spacing is relatively insensitive to whether the cylinders are isothermal or with uniform heat flux.

1. INTRODUCTION

In this paper we report the results of a theoretical, numerical and experimental study of how to determine the optimal spacing for horizontal cylinders in an array with natural convection heat transfer. The volume occupied by the array is fixed. The number of cylinders in the array, or the spacing between cylinders of fixed diameter, can vary. The optimal spacing reported in this paper corresponds to the maximum overall heat transfer (or thermal conductance) between the array and the surrounding fluid.

The optimal spacing question is both important and timely. It is important because of its obvious implications in the design of heat exchangers, surfaces with horizontal pin fins, and, generally, the cooling by natural convection of a space of fixed size (e.g. electronic package). The question is timely in view of the large volume of research that has been devoted to arrays of horizontal cylinders with natural convection on the outside. This body of work was reviewed on several occasions (e.g. Guceri and Farouk [1]; Sadeghipour and Asheghi [2]) and will not be reviewed here. Most of this work dealt primarily with the detailed interaction between adjacent cylinders (e.g. Marsters [3]; Farouk and Guceri [4]), not with the overall performance (thermal conductance) of the entire array.

The existence of an optimal spacing for maximum heat transfer was noted by Sparrow and Vemuri [5] in an experimental study of an array with a large number of horizontal pin fins. The heat transfer was by combined natural convection and radiation. The maximum exhibited by the overall heat transfer rate was very shallow and corresponded to using an array with approximately 35 pin fins.

Related aspects of this subject were considered by Tokura *et al.* [6] and Sadeghipour and Asheghi [2]. Tokura *et al.* reported an optimal spacing for a vertical column of horizontal cylinders confined by two vertical plates. It is not at all clear, however, that their result corresponds to maximum heat transfer. Their recommendation to use six cylinders in the array appears to be a trade-off between transferring more heat and using more hardware (cylinders).

Sadeghipour and Asheghi reconsidered the optimal spacing question in Tokura *et al.*'s configuration. Their experimental results suggest a shallow maximum in the variation of the overall heat transfer

NOMENCLATURE

D	diameter	S	cylinder-to-cylinder spacing
g	gravitational acceleration	$\bar{S}$	volume averaged spacing
H	height of array, Fig. 1	T	temperature
k	thermal conductivity	T_w	cylinder surface temperature
L	cylinder length, Fig. 1	T_∞	coolant inlet temperature
n	number of cylinders in the volume HLW	u, v	velocity components
		U, V	dimensionless velocity components
n_c	number of half-cylinders in the computational domain	U	mean velocity through $\bar{S}$-wide channel
		W	frontal width of array, Fig. 1
Nu_D	single cylinder overall Nusselt number	x, y	horizontal and vertical coordinates
p	pressure	X, Y	dimensionless coordinates.
P	dimensionless pressure		
Pr	Prandtl number, ν/α		
q_1	heat transfer from a single cylinder	Greek symbols	
q	heat transfer from the entire array	α	thermal diffusivity
$\tilde{q}$	dimensionless heat transfer volumetric density	β	coefficient of volumetric thermal expansion
Ra_D	Rayleigh number, $g\beta D^3(T_w-T_\infty)/(\alpha\nu)$	θ	dimensionless temperature
Ra_H	Rayleigh number, $g\beta H^3(T_w-T_\infty)/(\alpha\nu)$	ρ	density.

rate with the cylinder-to-cylinder spacing. The final correlation for this relationship, however, does not indicate a maximum with respect to spacing: the overall heat transfer increases monotonically with the spacing, and reaches its highest values (or plateau) when the S/D ratio exceeds approximately 15.

The absence of a correlation for the reported optimal spacings, and the inability to predict optimal spacings in new configurations defined the objectives of the present study. To begin with, we focused exclusively on heat transfer by natural convection (without radiation). Our objective was not only to determine the optimal spacings for various situations, but also to correlate our results in a compact dimensionless relation valid for any array with laminar natural convection.

To achieve this objective we conducted the study in three phases. In the first, we developed a pure theory to prove the existence of the optimal spacing, and to reveal the proper dimensionless groups and analytical form of the optimal-spacing correlation. In the second phase, we simulated the natural convection flow and temperature fields, and varied the spacing (or number of cylinders) of the array to generate optimal-spacing data to be correlated based on the theory. Finally, in the third phase of the study we experimented with several arrays of cylinders that occupied the same volume. The purpose of these experiments was to determine the optimal spacing through direct heat transfer and temperature measurements, and to test in this way the accuracy of the numerical phase of the study.

2. THEORETICAL RESULTS

We begin with a theoretical argument to demonstrate that there exists an optimal cylinder-to-cylinder spacing for maximum heat transfer, and to identify the proper dimensionless groups needed to correlate the optimal spacing results determined more accurately (numerically and experimentally).

Consider the bundle of horizontal cylinders shown in Fig. 1. The overall dimensions of the bundle (H, L, W) and the cylinder diameter (D) are fixed. Natural convection heat transfer (q) occurs between the cylinder surfaces (T_w) and the surrounding fluid reservoir (T_∞). In the following analysis we address the question of how to select the number of cylinders in the bundle, or the cylinder-to-cylinder spacing (S), such that the *overall* thermal conductance between the bundle and the ambient, $q/(T_w-T_\infty)$ is maximized. For the sake of conciseness we assume that the cylinders are staggered, and that their centers form equilateral triangles. Other array types can be treated similarly. The problem is similar to that of determining

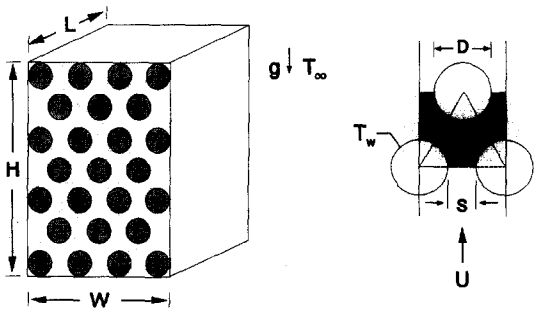

Fig. 1. Bundle of horizontal cylinders immersed in a quiescent fluid (a), and detail of one of the channels traveled by the fluid (b).

the optimal number of plates in a stack cooled by natural or forced convection [7–11].

When the spacing S and the Rayleigh number are sufficiently large, each horizontal cylinder is coated by a distinct boundary layer, and the surrounding fluid is at the temperature T_∞. We are assuming that $(H, W) \gg (D+S)$, and that $Ra_D \gg 1$, where $Ra_D = g\beta D^3(T_w - T_\infty)/(\alpha\nu)$. The heat transfer from one cylinder is

$$q_1 \cong \frac{k}{D} Nu_D \pi DL (T_w - T_\infty) \tag{1}$$

where the overall Nusselt number is (cf. Morgan [12], $10^4 < Ra_D < 10^7$)

$$Nu_D = 0.48\, Ra_D^{1/4}. \tag{2}$$

The total number of cylinders in the bank of cross-sectional area $H \times W$ is

$$n = \frac{HW}{(S+D)^2 \cos 30^\circ} \tag{3}$$

therefore the total heat transfer from the bank is $q = nq_1$ or

$$q_{\text{large S}} \cong 1.74 \frac{HLW}{(S+D)^2} k(T_w - T_\infty) Ra_D^{1/4}. \tag{4}$$

This result shows that, when the spacing is large, the overall thermal conductance $q/(T_w - T_\infty)$ decreases as S increases.

Consider now the opposite extreme when the cylinders almost touch, and the flow is almost cut off. In this limit the temperature of the coolant that exits slowly through the upper plane of the bundle $(L \times W)$ is essentially the same as the cylinder temperature T_w. The heat transfer from the bundle to the coolant is equal to the enthalpy gained by the coolant, $q = \dot{m} c_p (T_w - T_\infty)$, where $\dot{m}$ is the mass flow rate through the $L \times W$ plane.

To obtain an order-of-magnitude estimate for the flow rate, we note that $\dot{m}$ is composed of several streams [total number $= W/(S+D)$], each with a cross-sectional area $S \times L$ in the plane of one horizontal row of cylinder axes. The thickness of the channel traveled upward by each stream varies between a minimum value (S) at the row level, and a maximum value at a certain level between two rows. The volume-averaged thickness of one channel is

$$\bar{S} = S + D - 0.907 \frac{D^2}{S+D} \tag{5}$$

however, we may adjust this estimate by using 1 in place of the factor 0.907 to account for the fact that the channel closes (i.e. the flow must stop) when the cylinders touch ($S = 0$)

$$\bar{S} = S \frac{S+2D}{S+D}. \tag{6}$$

When $\bar{S}$ is sufficiently small, the flow rate through each channel of cross sectional area $\bar{S}L$ and flow length H is proportional to the pressure difference that drives the flow. The pressure difference is $\Delta P = \rho g H \beta (T_w - T_\infty)$, or the difference between the hydrostatic pressures under two H-tall columns of coolant, one filled with T_∞ fluid, and the other with T_w fluid. The mean velocity of the channel flow, U, can be approximated using the Hagen–Poiseuille solution for flow between two parallel plates (spacing $\bar{S}$, flow length H),

$$U = \frac{\bar{S}^2 \Delta P}{12 \mu H}. \tag{7}$$

The total flow rate through the bundle, $\dot{m}(\rho U \bar{S} L) \cdot W/(S+D)$, leads to the total heat transfer rate $\dot{m} c_p (T_w - T_\infty)$, which can be summarized as

$$q_{\text{small S}} \cong \frac{\bar{S}^3 LW}{12 D^3 (S+D)} k(T_w - T_\infty) Ra_D. \tag{8}$$

The key feature of this estimate is that when S is small and decreases, the thermal conductance $q/(T_w - T_\infty)$ decreases as S^3.

Figure 2 summarizes the trends uncovered so far. The actual thermal conductance would be represented by the solid curve sketched in the figure. The peak of this curve corresponds to a spacing (S_{opt}) that can be approximated by intersecting the two asymptotes [7, 11], $q_{\text{large S}} = q_{\text{small S}}$. The result of eliminating q between equations (4) and (8) is

$$\frac{S_{opt}}{D} \cdot \frac{2 + S_{opt}/D}{(1 + S_{opt}/D)^{2/3}} \cong 2.75 \left(\frac{H}{D}\right)^{1/3} Ra_D^{-1/4}. \tag{9}$$

This relation is plotted in Fig. 3, which shows that S_{opt}/D is almost proportional to the group $(H/D)^{1/3} Ra_D^{-1/4}$. In other words, a simpler alternative to the order of magnitude estimate obtained in equation (9) is

$$\frac{S_{opt}}{D} \sim \left(\frac{H}{D}\right)^{1/3} Ra_D^{-1/4} \tag{10}$$

or

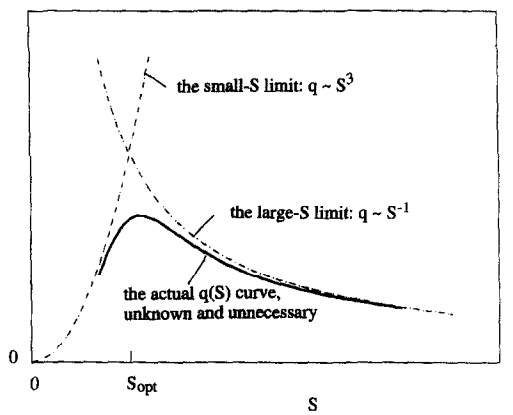

Fig. 2. The optimal cylinder-to-cylinder spacing for maximum thermal conductance, as the intersection of the large- and small-S asymptotes.

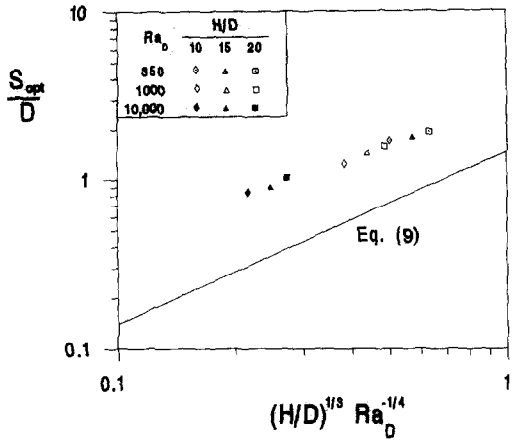

Fig. 3. The optimal cylinder-to-cylinder spacing as a function of bundle height and cylinder diameter ($Pr = 0.72$).

$$\frac{S_{opt}}{H} \sim \left(\frac{H}{D}\right)^{1/12} Ra_H^{-1/4} \tag{11}$$

where $Ra_H = g\beta H^3(T_w - T_\infty)/(\alpha\nu)$. Equation (11) shows that the optimal spacing is approximately proportional to $H^{1/3}D^{-1/12}$, which means that it is almost insensitive to changes in the cylinder diameter.

3. NUMERICAL RESULTS

In this section and the next we report numerical and experimental results for the optimal cylinder-to-cylinder spacing. The objective of these empirical phases of our study was to test and improve the accuracy of the correlation determined theoretically, equations (9)–(11).

The natural convection and heat transfer in an array of horizontal cylinders was simulated numerically by focusing on a vertical channel formed between two adjacent rows of cylinders, Fig. 4. It was assumed that the flow is laminar, such that there is no exchange of fluid and energy between adjacent channels. The regime is laminar when $Ra_H \leqslant 10^9 Pr$ (Bejan and Lage [13], because H is the relevant vertical dimension of the channel with boundary layer flow.

The mass, momentum and energy equations were simplified in accordance with the assumptions of two-dimensional steady state, nearly constant properties, and Boussinesq approximation in the buoyancy term of the momentum equation for the vertical (y) direction

$$\frac{\partial u}{\partial x} + \frac{\partial v}{\partial y} = 0 \tag{12}$$

$$u\frac{\partial u}{\partial x} + v\frac{\partial u}{\partial y} = -\frac{1}{\rho}\frac{\partial p}{\partial x} + \nu\nabla^2 u \tag{13}$$

$$u\frac{\partial v}{\partial x} + v\frac{\partial v}{\partial y} = -\frac{1}{\rho}\frac{\partial p}{\partial y} + \nu\nabla^2 v + g\beta(T - T_\infty) \tag{14}$$

$$u\frac{\partial T}{\partial x} + v\frac{\partial T}{\partial y} = \alpha\nabla^2 T \tag{15}$$

where $\nabla^2 = \partial^2/\partial x^2 + \partial^2/\partial y^2$. The horizontal and vertical velocity components are u and v. The origin of the Cartesian frame (x, y) is located in the bottom left corner of the computational domain. The computational domain contains the actual channel of height H/D (fixed), plus an inlet (bottom) section and an outlet (top) section. Accuracy tests showed that when the inlet length is $2.5D$ and the outlet length $3D$, the calculated heat transfer from the channel is insensitive (with changes less than 1%) to further doubling of the inlet and outlet lengths.

The flow boundary conditions were: zero normal stress and vertical flow ($u = 0$) at the inlet to the computational domain ($x = 0$); free slip and no penetration at the fluid interfaces (planes of symmetry) between two consecutive cylinders; no slip and no penetration at the cylinder surfaces, and free slip and no penetration on the vertical boundaries of the inlet section. It is important to note that the forcing of free slip and no penetration conditions on the vertical boundaries of the outlet section would induce an artificial acceleration of the fluid (updraft, chimney effect) through the cylinder-to-cylinder channel. To avoid this effect, a zero stress inlet condition was specified along one of the sides of the outlet section, specifically, on the side opposite the topmost cylinder (Fig. 4).

The temperature boundary conditions were $T = T_w$ on the cylinder surfaces, and $T = T_\infty$ at the bottom end of the computational domain. The remaining portions of the boundary of the computational domain were modelled as adiabatic.

Equations (12)–(15) were nondimenionalized by defining the dimensionless variables

$$(X, Y) = \frac{(x, y)}{D} \quad (U, V) = \frac{(u, v)}{(\alpha/D)(Ra_D Pr)^{1/2}} \tag{16}$$

$$\theta = \frac{T - T_\infty}{T_w - T_\infty} \quad P = \frac{pD^2}{\mu\alpha(Ra_D Pr)^{1/2}}. \tag{17}$$

Numerical solutions were generated for $Pr = 0.72$. The system of equations was solved on a Cray-YMP using a finite element package [14]. Grid refinement tests showed that 40 nodes per D in x and y were necessary for $Ra_D = 10^4$, such that the further doubling of the number of nodes caused a change of less than 2% in the heat flux from each cylinder.

The accuracy of the numerical method was checked further by placing a single half cylinder in the computational domain, and calculating the overall Nusselt number Nu_D. The values obtained were $Nu_D = 3.20$ for $Ra_D = 10^3$, and $Nu_D = 5.10$ for $Ra_D = 10^4$. These values agree within 6% with the large body of empirical results compiled by Morgan [12], and fall between the error bars indicated by Morgan for the correlation listed in equation (2).

For each array geometry (H/D, S/D) the solutions were generated by solving for $Ra_D = 10^3$ first, and then using that solution as initial condition for the next higher Ra_D. The computational time depended strongly on the array geometry and Rayleigh number.

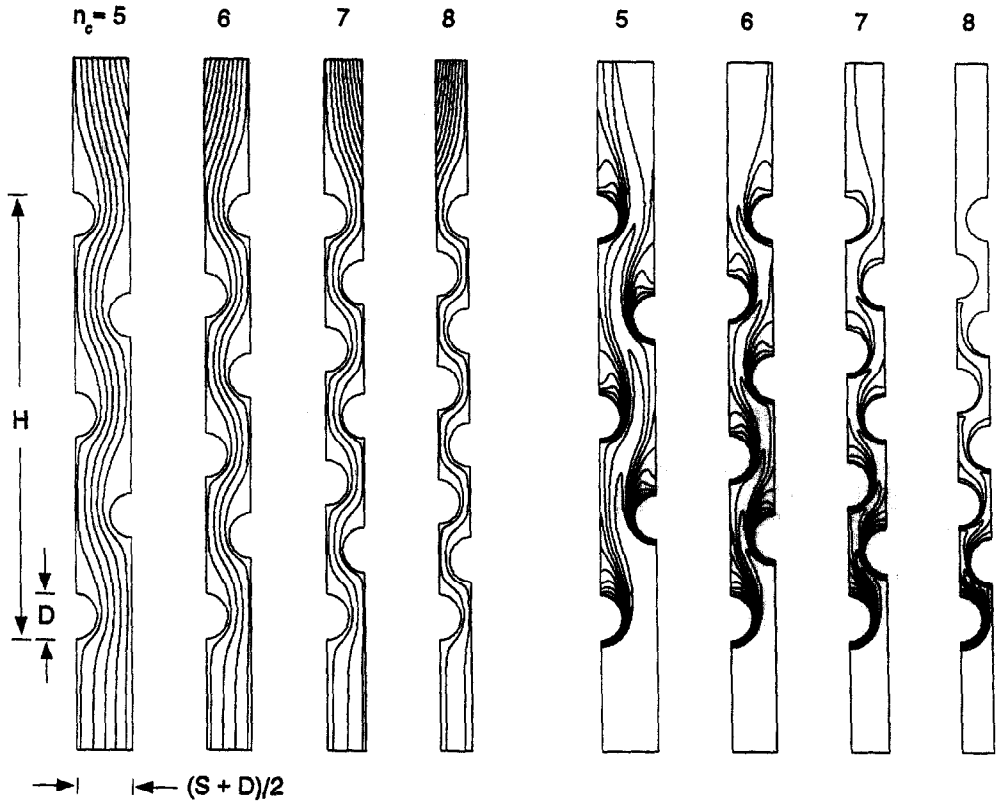

Fig. 4. The computational domain, and the effect of cylinder-to-cylinder spacing on the flow and temperature fields ($H/D = 10$, $Ra_D = 10^4$, $Pr = 0.72$). The streamlines are on the left, and isotherms on the right.

Figure 4 shows a sample of the flow and temperature fields calculated for $H/D = 10$ and $Ra_D = 10^4$. The streamline and isotherm patterns are arranged in a way that illustrates our search for the optimal cylinder-to-cylinder spacing of an array in a *fixed volume*. We fixed the height of the array (H), and decreased the spacing (S): we did this discretely (in steps), each time by adding one more to the number of cylinders (n_c) in the channel of height H.

During this sequence we monitored the total heat transfer from all the half-cylinders, to see how it responds to changes in S. A sample is shown in Fig. 5, where the ordinate parameter represents the dimensionless heat transfer volumetric density,

$$\tilde{q} = \frac{q}{HLW}\frac{D^2}{k(T_w - T_\infty)} \tag{18}$$

where q is the total heat transfer from an array of fixed volume HLW. Figure 5 shows that there is an optimal spacing for maximum heat transfer. The S_{opt}/D values were determined by fitting the highest three $\tilde{q}$ points with a parabola, and solving $\partial\tilde{q}/\partial(S/D) = 0$. The best practical spacing, of course, corresponds to the number of cylinders n (an integer) that maximizes the total heat transfer rate from the given space.

The resulting S_{opt}/D data are reported in Fig. 3.

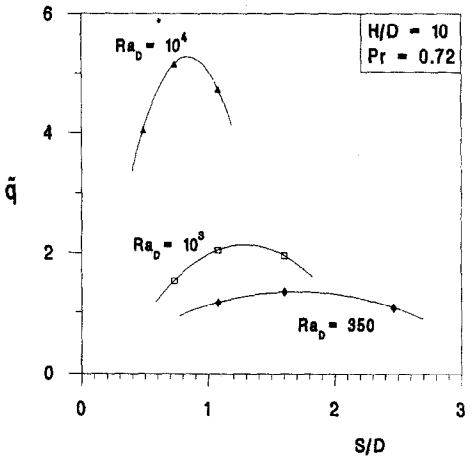

Fig. 5. The effect of the cylinder-to-cylinder spacing on the total heat transfer from the array ($H/D = 10$, $Pr = 0.72$).

They are correlated very nicely in the manner anticipated in Section 2, namely by using the group $(H/D)^{1/3}Ra_D^{-1/4}$ on the abscissa. The optimal spacings, however, are consistently 2.5 times larger than the values calculated based on equation (9). The function of type (10) that fits the numerical data the best (within 1.7% mean error) is

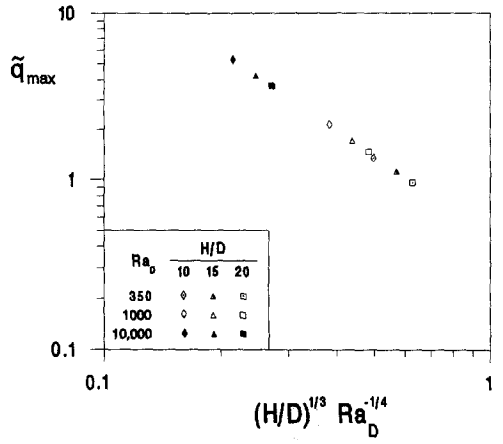

Fig. 6. The maximum array heat transfer rate, or maximum heat transfer volumetric density, corresponding to the numerical optimal spacing data of Fig. 3.

$$\frac{S_{opt}}{D} = 2.72\left(\frac{H}{D}\right)^{1/3} Ra_D^{-1/4} + 0.263 \qquad (19)$$

where 0.263 is a small correction term.

The maximum heat transfer density that corresponds to the optimal spacing of Fig. 3 is reported in Fig. 6. The dimensionless group used on the abscissa of Fig. 6 is the result of the theory: it is easy to show that when equation (19) is substituted without the 0.263 correction into equation (4) or equation (8), the group $\tilde{q}/Ra_D^{1/4}$ becomes a function of only the group $(H/D)^{1/3}Ra_D^{-1/4}$, which appeared also on the abscissa of Fig. 3. The numerical data, however, are correlated better if we plot $\tilde{q}$ instead of $\tilde{q}/Ra_D^{1/4}$ on the ordinate. The data shown in Fig. 6 are reproduced within 1.7% by the correlation

$$\tilde{q}_{max} = 0.448\left[\left(\frac{H}{D}\right)^{1/3} Ra_D^{-1/4}\right]^{-1.6}. \qquad (20)$$

4. EXPERIMENTAL RESULTS

Figure 7 shows the main features of the arrays used in the experimental phase of this study. The array volume was fixed: $H = 39.4$ mm, $L = 142$ mm and $W = 44.5$ mm. Three arrays were constructed by varying from 5 to 3 the number of horizontal rows in the $H \times W$ cross-section. The number of cylinders of the three arrays were 23, 14 and 8, and the respective spacings S/D were 0.5, 1 and 2.

The apparatus construction and measurement technique retained many of the features described by Marsters [3]. The longitudinal conduction and loss of heat through the cylinder ends were minimized by holding each cylinder between two vertical wooden walls. The array assembly was held inside a 2 m-high enclosure with a horizontal cross-section of 0.4×0.4 m. The bottom and top ends of the enclosure were open to room air. To reduce the effect of radiation, the internal and external surfaces of the enclosure were covered with aluminum foil. By using the method of calculation outlined in Morgan [12] and Sadeghipour and Asheghi [2], we estimated that in our experiments the radiation contribution to the overall heat transfer rate was less than 1.6%. The maximum temperature recorded on the array (T_{w1}, Fig. 7) was 47.2°C.

Each cylinder was a low density electrical heater consisting of a helically wound heating element (resistance 96 Ω) held in a ceramic insulator filled with conductive magnesium oxide. The outer cover was polished 304 stainless steel, which provided adequate rigidity and resistance to oxidation. The heaters were connected in parallel, and powered by a variable autotransformer that produced a voltage between 0 and 140 V.

The temperatures T_{w1}, T_{w2} and T_∞ were measured in the vertical midplane of the array, i.e. half-way between the two wooden walls. Copper–constantan type T thermocouples were imbedded in 1 mm hemispherical depressions machined into the stainless steel sheath of the heater. The thermocouple readings were referenced to a mixture of crushed ice and water. As the heat transfer rate per cylinder was distributed uniformly throughout the array, the maximum temperature was registered on the trailing row of cylinders (T_{w1}). The temperature was practically uniform (within 0.04°C) around the cylinder circumference: we measured this variation by running experiments with a single cylinder, and rotating the cylinder to change the position of the thermocouple on the circumference.

The overall thermal conductance $\tilde{q}$ was calculated after measuring the power dissipated in all the heaters (q), the maximum temperature (T_{w1}) and the room temperature at the bottom (inlet) of the enclosure (T_∞). The $\tilde{q}$ values were calculated using T_{w1} in place of T_w in equation (18). The properties of air were evaluated at the average temperature $(T_w + T_\infty)/2$, where $T_w = (T_{w1} + T_{w2})/2$.

The uncertainties associated with the $\tilde{q}$ and Ra_D values determined in this manner were 2.5 and 4.9%, respectively. These were estimated based on the method of Kline and McClintock [15], and the following inputs: 0.84% uncertainty in T_{w1}, T_{w2} and T_∞, resulting from the calibration of the thermocouples; 0.5 and 1% uncertainties in the measurement of voltage and current, respectively; and 0.28% for c_p, 2% for μ and 1% for k (listed in ref. [16]).

We started each run by setting the voltage and current for the resistance heaters. We then waited 3–4 h while monitoring the changes in voltage, current, T_{w1}, T_{w2} and T_∞. We ended the run by taking final readings when the relative change in voltage, current and temperature readings was less than 0.2%, 0.2% and 0.06% (determined by repeating 10 h-long runs at the same spacing and Ra_D), respectively. These relative changes are small when compared with the uncertainties in the respective measurements.

Figure 8 shows a summary of the heat transfer experiments. The figure shows also the curve fitting

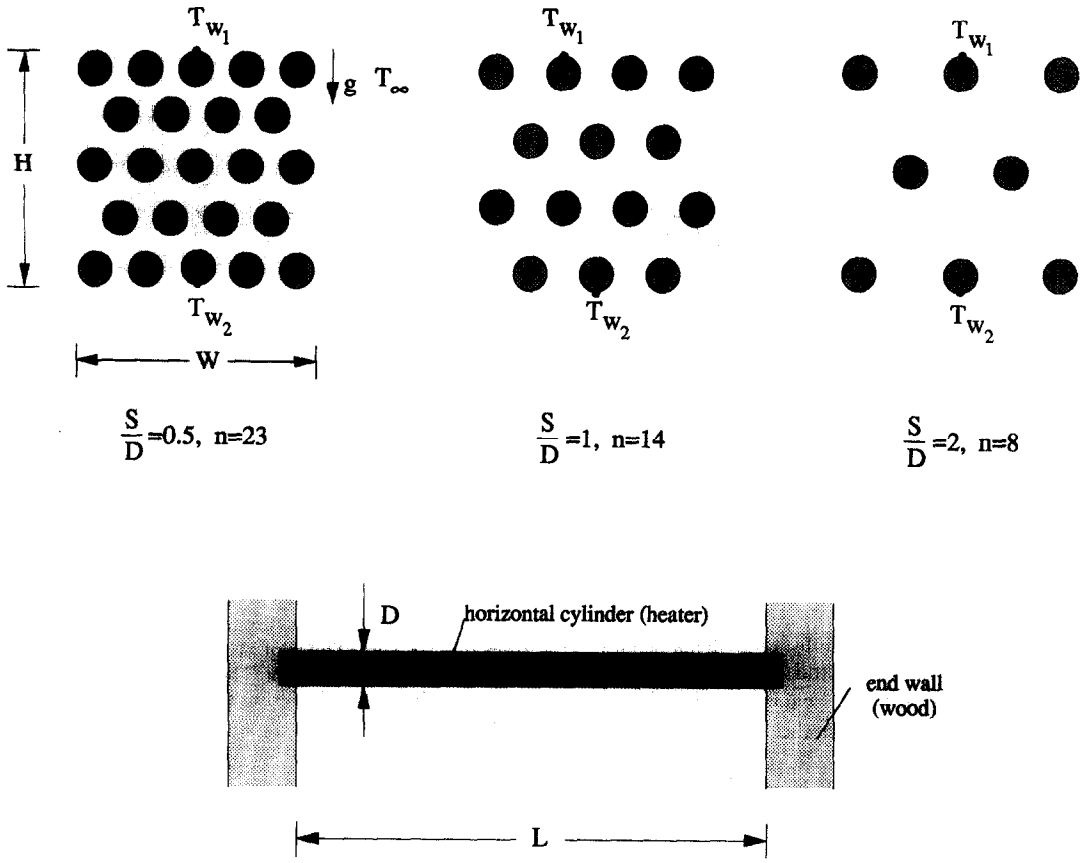

Fig. 7. Details of the test section of the experimental apparatus.

procedure used for determining S_{opt}/D, i.e. the same procedure as in the numerical part of the study (Fig. 5). The optimal spacings calculated in this manner are reported in Table 1. Again, the best practical array is the one with the largest overall thermal conductance, namely the case $n = 14$ (Figs. 7 and 8). The curve fitting of the $\tilde{q}$ data in Fig. 8 is used only as a test of the accuracy of the method employed in the numerical part of the study.

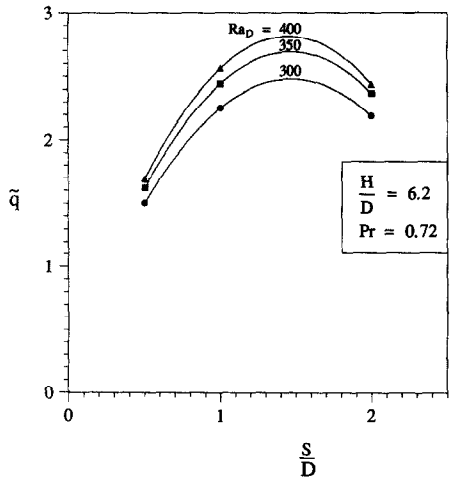

Fig. 8. Experimental results for the total heat transfer rate from the array ($H/D = 6.2$, $Pr = 0.72$).

We used these experimental results to verify the accuracy of the numerical method described in the preceding section. The numerical results have been added to Table 1. We performed the numerical work for $H/D = 6.2$ and $Pr = 0.72$, which correspond to the experimental conditions. First, we modelled the cylinders as surfaces with uniform flux, and found that the maximum temperature occurs at the top of the topmost cylinder. The optimal spacing determined numerically agrees within 17% with the corresponding experimental result.

We used this opportunity to see if the type of cylinder thermal boundary condition has an effect on the optimal spacing. We solved again the experimental configuration numerically, this time modelling the cylinders as isothermal, and found the results listed in the bottom line of Table 1. In place of T_w in equation (18) we used the average temperature of the topmost cylinder. It is clear that the optimal spacing is relatively insensitive to whether the array is uniform-flux or isothermal. This conclusion is important, because it means that the corelation (19) is general.

Additional evidence that the present results are correct is provided by the experimental study of Sparrow and Vemuri [5]. As pointed out in the Introduction,

Table 1. Comparison between the optimal spacings determined experimentally, and the corresponding results obtained based on numerical simulations ($H/D = 6.2$, $Pr = 0.72$)

S_{opt}/D	Ra_D			
	200	300	350	400
Experiments		1.44	1.47	1.45
Numerical, uniform flux cylinders	1.78	1.68	1.62	1.61
Numerical, isothermal cylinders	1.54	1.48	1.46	1.44

Sparrow and Vemuri maximized the total heat transfer rate from an isothermal vertical plate ($H = W = 7.62$ cm) with horizontal pin fins ($D = 0.635$ cm). Because the heat transfer maximum was rather flat, Sparrow and Vemuri concluded that the optimal spacing occurs when the total number of pins fins is between 30 and 40. The flat maximum was observed at Rayleigh numbers (based on H) in the range 4×10^5–16×10^5.

Translated into the terminology employed in the present study, Sparrow and Vemuri's conclusion means that the optimal spacing is in the range $1.04 < S_{opt}/D < 1.35$, when the Rayleigh number is in the range $230 < Ra_D < 920$. Their S_{opt}/D estimate agrees very well (within 10%) with the present experimental results (Table 1). This is remarkable, especially if we recognize that (i) the H/D ratios were different (12 for Sparrow and Vemuri, vs 6.2 in the present study), (ii) in their experiments radiation was important and (iii) their cylinders (pin fins) conducted heat longitudinally.

5. CONCLUSIONS

In this paper we developed fundamental results for the selection of the spacing between horizontal cylinders in an array of fixed volume. The heat transfer is by laminar natural convection. The optimal spacing reported in equation (19) corresponds to the maximum thermal conductance between the entire array and the surrounding fluid.

More important fundamentally is the conclusion that the optimal spacing and maximum thermal conductance can be expressed in compact dimensionless relations. The relevant dimensionless groups have been identified, and each relation contains only two groups: S_{opt}/D and $(H/D)^{1/3} Ra_D^{-1/4}$ for optimal spacing, equation (19), and $\tilde{q}_{max}$ and $(H/D)^{1/3} Ra_D^{-1/4}$ for maximum thermal conductance, equation (20).

These developments were possible only because we began the study with a purely theoretical look at the problem of predicting the optimal spacing. It was only after the theory that we resorted to empiricism (numerical and experimental), which was necessary in order to improve the accuracy of the theoretical expressions found for S_{opt}/D and $\tilde{q}_{max}$. Furthermore, the dimensionless groups and analytical expressions revealed by the theory had the effect of minimizing the amount of numerical and experimental information needed for developing the recommended results, equations (19) and (20).

The corresponding problem of optimizing the cylinder spacing in an array with *forced convection* is treated in a new book [17].

Acknowledgement—This work was supported by a grant from the Air Force Office of Scientific Research under the guidance of Major Dan Fant. The computational work was made possible by a grant from the North Carolina Supercomputing Center.

REFERENCES

1. S. Guceri and B. Farouk, Numerical solutions in laminar and turbulent natural convection. In *Natural Convection Fundamentals and Applications* (Edited by S. Kakac, W. Aung and R. Viskanta), pp. 615–654. Hemisphere, Washington D.C. (1985).
2. M. S. Sadeghipour and M. Asheghi, Free convection heat transfer from arrays of vertically separated horizontal cylinders at low Rayleigh numbers, *Int. J. Heat Mass Transfer* **37**, 103–109 (1994).
3. G. F. Marsters, Arrays of heated horizontal cylinders in natural convection, *Int. J. Heat Mass Transfer* **15**, 921–933 (1972).
4. B. Farouk and S. I. Guceri, Natural convection from horizontal cylinders in interacting flow fields, *Int. J. Heat Mass Transfer* **26**, 231–243 (1983).
5. E. M. Sparrow and S. B. Vemuri, Natural convection/radiation heat transfer from highly populated pin fin arrays, *J. Heat Transfer* **107**, 190–197 (1985).
6. I. Tokura, H. Saito, K. Kishinami and K. Muramoto, An experimental study of free convection heat transfer from a horizontal cylinder in a vertical array set in free space between parallel walls, *J. Heat Transfer* **105**, 102–107 (1983).
7. A. Bejan, *Convection Heat Transfer*, Chap. 4, Problem 11. Wiley, New York (1984).
8. A. Bar-Cohen and W. M. Rohsenow, Thermally optimum spacing of vertical, natural convection cooled, parallel plates, *J. Heat Transfer* **106**, 116–123 (1984).
9. S. H. Kim, N. K. Anand and L. S. Fletcher, Free convection between series of vertical parallel plates with embedded line heat sources, *J. Heat Transfer* **113**, 108–115 (1991).
10. N. K. Anand, S. H. Kim and L. S. Fletcher, The effect of plate spacing on free convection between heated parallel plates, *J. Heat Transfer* **114**, 515–518 (1992).
11. A. Bejan and E. Sciubba, The optimal spacing of parallel plates cooled by forced convection, *Int. J. Heat Mass Transfer* **35**, 3259–3264 (1992).

12. V. T. Morgan, The overall convective heat transfer from smooth circular cylinders, *Adv. Heat Transfer* **11**, 199–264 (1975).
13. A. Bejan and J. L. Lage, The Prandtl number effect on the transition in natural convection along a vertical surface, *J. Heat Transfer* **112**, 787–790 (1990).
14. FIDAP, Theoretical Manual, V.6.03. Fluid Dynamics International, Evanston, IL (1991).
15. S. J. Kline and F. A. McClintock, Describing uncertainties in single-sample experiments, *Mech. Engng* **3**, Jan. (1953).
16. *Thermophysical Properties of Matter*, TPRC, Vols 3, 6 and 11, Data Series, Purdue Research Foundation, New York (1970).
17. A. Bejan, *Convection Heat Transfer*, 2nd edn, Problems 3.25 and 4.29. Wiley, New York (1995).